Automatica 47 (2011) 85–91

Contents lists available at ScienceDirect

Automatica

journal homepage: www.elsevier.com/locate/automatica

Brief paper

Navigation of a unicycle-like mobile robot for environmental extremum seeking☆

Alexey S. Matveev [a,*], Hamid Teimoori [b], Andrey V. Savkin [b]

[a] Department of Mathematics and Mechanics, Saint Petersburg University, Universitetskii 28, Petrodvoretz, St. Petersburg, 198504, Russia

[b] School of Electrical Engineering and Telecommunications, The University of New South Wales, Sydney 2052, Australia

ARTICLE INFO

Article history:
Received 7 October 2009
Received in revised form
31 May 2010
Accepted 5 August 2010
Available online 20 November 2010

Keywords:
Non-holonomic vehicles
Navigation
Gradient climbing
Source seeking
Sliding mode control

ABSTRACT

We consider a single Dubins-like mobile robot traveling with a constant longitudinal speed in a planar region supporting an unknown field distribution. A single sensor provides the distribution value at the current robot location. We present a new sliding mode navigation strategy that drives the robot to the location where the field distribution attains its maximum. The proposed control algorithm does not employ gradient estimation and is non-demanding with respect to both computation and motion. Its mathematically rigorous analysis and justification are provided. Simulation results confirm the applicability and performance of the proposed guidance approach.

1. Introduction

In this paper, we consider the problem of steering a single non-holonomic mobile robot to the extrema of an unknown scalar environmental field. This field may represent the strength of a spatially distributed signal, e.g., an electromagnetic or acoustic one, the concentration of a chemical, physical or biological agent, the distribution of a physical quantity, such as thermal, magnetic, electric, or optical field distributions, etc. Examples of missions where steering to extrema is of interest include environmental studies, detecting and localizing the sources of hazardous chemicals leakage or vapor emission, sources of pollutants and plumes, hydrothermal vents, etc. In the literature, the problems of such a kind are basically referred to as those of source seeking/localizing (Cochran & Krstic, 2009; Porat & Neohorai, 1996; Zhang, Arnold, Ghods, Siranosian, & Krstic, 2007) or gradient climbing/descent/ascent (Bachmayer & Leonard, 2002; Biyik & Arcak, 2007; Burian, Yoeger, Bradley, & Singh, 1996; Ögren, Fiorelli, & Leonard, 2004). In the first case, the field distribution is caused by emission of some substance from a pointwise source at which location the distribution attains its maximum. The second name stresses that the maximum search is via ensuring constant increase of the distribution value at the vehicle location, with the best option being to move in the direction of the field gradient.

In recent decades, an extensive body of research has been devoted to sensor-based motion control for source seeking/gradient climbing; see e.g., Biyik and Arcak (2007), Cochran and Krstic (2009) and Ögren et al. (2004) and the references therein. Most of the proposed approaches employ on-line estimation of the gradient at the current location. Mobile sensor networks, which have enjoyed much attention recently (Bachmayer & Leonard, 2002; Biyik & Arcak, 2007; Gazi & Passino, 2004; Ögren et al., 2004; Porat & Neohorai, 1996), acquire extended capabilities for gradient estimation thanks to collaborative field sensing and data exchange. The single robot scenario is more challenging in this respect, unless the robot is equipped with numerous sensors providing the distribution values at various locations. If multiple sensor information is unavailable, a typical method to compensate for the lack of data is to get extra information via special maneuvers by 'dithering' the sensor position (Burian et al., 1996; Cochran & Krstic, 2009; Zhang et al., 2007). For example, in accordance with a general approach to the wider problem of extremum-seeking design (Ariyur & Krstic, 2003), the vehicle is excited with probing high-frequency sinusoidal inputs (Cochran & Krstic, 2009; Zhang et al., 2007).

In this paper, we propose a navigation law that is not based on intentional systematic exploration maneuvers but nevertheless steers a single mobile robot to the location where an unknown field distribution attains its maximum. Modulo natural and partly

☆ This work was supported by the Australian Research Council and the Russian Foundation for Basic Research, grants 08-01-00775 and 09-08-00803. The material in this paper was partially presented at 2010 American Control Conference, June 30–July 02, 2010, Baltimore, Maryland, USA. This paper was recommended for publication in revised form by Associate Editor Masayuki Fujita under the direction of Editor Ian R. Petersen.

* Corresponding author. Tel.: +7 812 4284148; fax: +7 812 4286944.
E-mail addresses: almat1712@yahoo.com (A.S. Matveev), h.teimoori@unsw.edu.au (H. Teimoori), a.savkin@unsw.edu.au (A.V. Savkin).

0005-1098/$ – see front matter © 2010 Elsevier Ltd. All rights reserved.
doi:10.1016/j.automatica.2010.10.003

unavoidable assumptions, the distribution is arbitrary. The robot is modeled as a unicycle, travels with a constant speed, and is controlled by the angular velocity limited by a given constant. A single sensor provides the distribution value at the robot location and the controller is able to acquire knowledge of the rate at which this measurement evolves over time, but no further sensing capabilities are assumed. Unlike the mainstream in the area, the proposed control law does not employ gradient estimates at the robot current location but originates from the equiangular navigation algorithm (Teimoori & Savkin, 2010). Mathematically rigorous justification of the control law is offered. We also describe a domain of the controller parameters for which the objective is achieved: the robot inevitably reaches the desired neighborhood of the maximum point for a finite time and remains there afterwards. The applicability of the proposed control law is confirmed by computer simulations.

The proposed strategy belongs to the class of sliding mode control laws (Utkin, 1992). Due to the well-known benefits such as high insensitivity to noises, robustness against uncertainties, good dynamic response, etc. (Utkin, 1992), the sliding mode approach is attracting a growing interest in the area of motion control. The major obstacle to implementation of sliding mode controllers is a harmful phenomenon called "chattering", i.e., undesirable finite frequency oscillations around the ideal trajectory due to unmodeled system dynamics and constraints. The problem of chattering elimination and reduction has an extensive literature (see Edwards, Fossas, and Fridman (2006) and Lee, Utkin, and Malinin (2009) for a survey). It offers a variety of effective approaches, including smooth approximation of the discontinuity, inserting low-pass filters/observers into the control loop, combining sliding mode and adaptive control or fuzzy logic techniques, higher-order sliding modes, etc. If chattering is encountered in applications of the proposed controller, it can be subjected to treatment under the framework of the above general discipline.

The body of the paper is organized as follows. Section 2 presents the system description and problem set-up, whereas Section 3 introduces and discusses assumptions. The main result is stated in Section 4. In Section 5, this result and the related controller design are illustrated for the simple yet instructive case of an isotropic distribution. All proofs are concentrated in Section 6 and the Appendix. Section 7 is concerned with simulation results.

2. System description and problem set-up

We consider a planar mobile robot modeled as a unicycle and controlled by the time-varying angular velocity u limited by a given constant $\overline{u}$. The robot travels with a constant speed v in an area hosting an unknown scalar field $D(\boldsymbol{r})$. Here $\boldsymbol{r} := \mathbf{col}\,(x, y)$ is the vector of the Cartesian coordinates x, y in the plane $\mathbb{R}^2$. The objective is to drive the robot to the point $\boldsymbol{r}^0$ where the field distribution $D(\boldsymbol{r})$ attains its maximum and then to keep it in a vicinity of $\boldsymbol{r}^0$, thus displaying the approximate location of the maximizer $\boldsymbol{r}^0$. The on-board control system has access only to the field value $d := D(x, y)$ at the robot current location $x = x(t), y = y(t)$ and the rate $\dot{d}$ at which this measurement evolves over time t. In particular, the entire gradient $\nabla D(x, y)$ is not accessible.

The kinematic model of the robot is as follows:

$$\begin{aligned} \dot{x} &= v\cos\theta, \\ \dot{y} &= v\sin\theta, \end{aligned} \qquad \dot{\theta} = u, \qquad |u| \le \overline{u}, \tag{1}$$

where θ gives the robot orientation. These equations are used to describe, for example, wheeled robots and missiles (see e.g. Manchester and Savkin (2004, 2006) and Teimoori and Savkin (2010) and the references therein). The problem is to design a controller that for a finite time t_0 drives the robot into the $R_\star$-neighborhood

$$V_\star := \{\boldsymbol{r} : \|\boldsymbol{r} - \boldsymbol{r}^0\| \le R_\star\} \tag{2}$$

of the maximizer $\boldsymbol{r}^0 : D(\boldsymbol{r}^0) = \max_{\boldsymbol{r}\in\mathbb{R}^2} D(\boldsymbol{r})$ and afterwards ($t \ge t_0$) keeps the robot within this neighborhood.

In this paper, we examine the following control algorithm:

$$u(t) = \overline{u}\ \mathrm{sgn}\,\{\dot{d}(t) - v_*\}, \tag{3}$$

where $v_* > 0$ is a tunable controller parameter.

3. Assumptions

In the above setting, the problem comprises the general problem of global optimization. As is well known, global optimization problems are typically quite difficult to solve. In the presence of local extrema, NP-hardness, the mathematical seal for intractability, was established for even the simplest classes of such problems (Horst & Pardalos, 1995). We do not mean to deal with NP-hard problems and impose the following assumption, which is realistic for many applications.

Assumption 3.1. The function $D(\cdot)$ is twice continuously differentiable. The maximum $\gamma_{\max} := \max_{\boldsymbol{r}\in\mathbb{R}^2} D(\boldsymbol{r})$ is attained at some point $\boldsymbol{r}^0$, which is the only critical point, i.e., $\nabla D(\boldsymbol{r}) \ne 0\ \forall \boldsymbol{r} \ne \boldsymbol{r}^0$. The set $\{\boldsymbol{r} \in \mathbb{R}^2 : D(\boldsymbol{r}) \ge \gamma_*\}$ is bounded whenever $\gamma_{\inf} := \inf_{\boldsymbol{r}\in\mathbb{R}^2} D(\boldsymbol{r}) < \gamma_* \le \gamma_{\max}$.

In many practical situations, $D(\boldsymbol{r}) \to \gamma_{\inf}$ as $\|\boldsymbol{r}\| \to \infty$. Then the last requirement from this assumption does indeed hold.

A good option in maximum seeking would be constant improvement of the robot position $\boldsymbol{r}(t)$ due to the monotone growth of the related field value $d(t) := D[\boldsymbol{r}(t)]$. The parameter v_* from (3) can be interpreted as the desired growth rate. However, even if the full data $\nabla D(\boldsymbol{r}), D(\boldsymbol{r}), \boldsymbol{r}, \theta$ are available, the control system is not always able to ensure the constant growth of d. To specify this, we introduce the following.

Definition 3.1. A point $\boldsymbol{r} \in \mathbb{R}^2$ is said to be *growth controllable* if, in any case of arrival at $\boldsymbol{r}$ with the field value d growing ($\dot{d} \ge 0$), the robot can maintain this growth by proper control u, provided that it is given access to the full data.

By (1), $\dot{d} = v[D'_x(\boldsymbol{r})\cos\theta + D'_y(\boldsymbol{r})\sin\theta]$ is a continuous function of time and is not immediately influenced by u. So, whenever $\dot{d} > 0$, the growth is 'automatically' maintained, irrespective of u. Hence, mathematically speaking, growth controllability means that $\dot{d} = 0 \Rightarrow \exists u \in [-\overline{u}, \overline{u}] : \ddot{d} \ge 0$.

The points outside a vicinity of the maximizer are typically growth controllable, as is implied by the following criterion.

Proposition 3.1. *A point $\boldsymbol{r}$ is growth controllable if and only if the (unsigned) curvature of the isoline*

$$I(\gamma) := \{\overline{\boldsymbol{r}} : D(\overline{\boldsymbol{r}}) = \gamma\} \tag{4}$$

passing through this point $\gamma := D(\boldsymbol{r})$ does not exceed the maximal turning curvature $\varkappa_{\mathrm{veh}} = \frac{\overline{u}}{v}$ of the robot whenever the isoline signed curvature $\varkappa(\boldsymbol{r})$ is negative:

$$-\varkappa_{\mathrm{veh}} \le \varkappa(\boldsymbol{r}) = \frac{\langle D''(\boldsymbol{r})\Phi_{\frac{\pi}{2}}\nabla D(\boldsymbol{r}); \Phi_{\frac{\pi}{2}}\nabla D(\boldsymbol{r})\rangle}{\|\nabla D(\boldsymbol{r})\|^3}. \tag{5}$$

The curvature sign corresponds to the case where the isoline is run so that greater values of D are to the right; in other words, the pair

of vectors $\nabla D, \dot{\boldsymbol{r}}$ is normally oriented. The curvature $\varkappa_{\text{veh}}$ is the reciprocal R^{-1} of the minimal turning radius $R = \frac{v}{\overline{u}}$ of the robot, and $\|\cdot\|$ and $\langle\cdot;\cdot\rangle$ stand for the standard norm and inner product in the Euclidian plane, whereas $D''(\boldsymbol{r})$ is the Hessian and Φ_α is the rotation matrix:

$$\Phi_\alpha := \begin{pmatrix} \cos\alpha & -\sin\alpha \\ \sin\alpha & \cos\alpha \end{pmatrix}. \tag{6}$$

The proof of Proposition 3.1 is given in the Appendix.

Isolines (4) with $\gamma \ll \max_{\boldsymbol{r}} D(\boldsymbol{r})$ typically are not very contorted. So growth uncontrollable points usually lie on isolines with $\gamma \approx \max_{\boldsymbol{r}} D(\boldsymbol{r})$, which, in total, form a small region around the maximizer $\boldsymbol{r}^0$.

To make the control objective realistic, it is natural to require that all points outside the desired vicinity (2) be growth controllable. Unavailability of $\nabla D(\boldsymbol{r})$ and θ for measurements, along with the need to keep the robot in the above vicinity, motivate enhancement of this requirement. To state it, we note that, thanks to Assumption 3.1,

$$\begin{aligned} &\gamma_\star := \max_{\boldsymbol{r}:\|\boldsymbol{r}-\boldsymbol{r}^0\|=R_\star} D(\boldsymbol{r}) < \gamma_{\max}, \\ &R_{\star\star} := \min_{\boldsymbol{r}:D(\boldsymbol{r})=\gamma_\star} \|\boldsymbol{r}-\boldsymbol{r}^0\| > 0. \end{aligned} \tag{7}$$

Assumption 3.2. The minimal turning radius $R = v/\overline{u}$ of the robot is less than $1/3R_{\star\star}$. All points $\boldsymbol{r}$ at a distance of no less than $R_{\star\star} - 2R$ from the maximizer are growth controllable: in other words, inequality (5) is true whenever $\|\boldsymbol{r}-\boldsymbol{r}^0\| \geq R_{\star\star} - 2R$. Moreover, this inequality holds with the strict inequality sign $>$ put in place of $\geq$.

4. Main result

We denote by C_{in} the circular trajectory of the robot driven by $u \equiv -\overline{u}$ from the given initial position, and put

$$\begin{aligned} &\gamma_{\text{in}} := \min_{\boldsymbol{r}\in C_{\text{in}}} D(\boldsymbol{r}), \\ &W := \{\boldsymbol{r}\in\mathbb{R}^2 : D(\boldsymbol{r}) \geq \min\{\gamma_{\text{in}}, \gamma_\star\}, \|\boldsymbol{r}-\boldsymbol{r}^0\| \geq R_{\star\star} - 2R\}, \end{aligned} \tag{8}$$

where $\gamma_\star$ is defined in (7). Due to the last claim from Assumption 3.1, the set W is compact, since $\gamma_{\text{in}}, \gamma_\star > \inf_{\boldsymbol{r}\in\mathbb{R}^2} D(\boldsymbol{r})$. (Otherwise, the point furnishing the minimum γ_{in} or $\gamma_\star$ would furnish $\min_{\boldsymbol{r}\in\mathbb{R}^2} D(\boldsymbol{r})$ and so would be critical, in violation of Assumption 3.1.)

Now we are in a position to state the main result of the paper.

Theorem 4.1. *Suppose that Assumptions 3.1 and 3.2 hold and that the parameter v_* of the controller (3) is chosen so that*

$$0 < v_* < v \min_{\boldsymbol{r}\in W} \|\nabla D(\boldsymbol{r})\|, \tag{9}$$

$$\begin{aligned} -\varkappa_{\text{veh}} \;<\; &\varkappa(\boldsymbol{r})\cos\alpha + \frac{\sin^2\alpha}{\cos\alpha}\frac{\langle D''(\boldsymbol{r})\nabla D(\boldsymbol{r});\nabla D(\boldsymbol{r})\rangle}{\|\nabla D(\boldsymbol{r})\|^3} \\ &- 2\sin\alpha\frac{|\langle D''(\boldsymbol{r})\Phi_{\frac{\pi}{2}}\nabla D(\boldsymbol{r});\nabla D(\boldsymbol{r})\rangle|}{\|\nabla D(\boldsymbol{r})\|^3} \quad \forall \boldsymbol{r}\in W, \end{aligned} \tag{10}$$

where $\alpha = \alpha(v_*, \boldsymbol{r}) := \arcsin\dfrac{v_*}{v\|\nabla D(\boldsymbol{r})\|}$ (11)

and the curvature $\varkappa(\boldsymbol{r})$ and the set W are given by (5) and (8), respectively. Then the robot driven by the controller (3) reaches the desired vicinity (2) of the maximizer for a finite time t_0 and remains there afterwards: $\boldsymbol{r}(t) \in V_\star$ for $t \geq t_0$.

The proof of this theorem will be given in Section 6.

Remark 4.1. (i) As $v_* \to 0$, the right-hand side of (10) converges to that of (5) uniformly over W. So, due to Assumption 3.2, (9) and (10) are satisfied if v_* is small enough. However, small v_* may worsen the transient performance: it is expected that $t_0 \uparrow$ as $v_* \downarrow$.

(ii) Practically, the choice of v_* is based on putting an upper estimate $\widehat{W}$ of W and estimates of the derivatives of $D(\cdot)$ involved in (9) and (10).

(iii) A way to follow the above lines is to first estimate the discrepancy in (5), i.e., to find $\Delta > 0$ such that

$$\varkappa(\boldsymbol{r}) \geq -\varkappa_{\text{veh}} + \Delta \quad \forall \boldsymbol{r}\in\widehat{W}. \tag{12}$$

Then we observe that, for $\boldsymbol{r}\in\widehat{W}$, (10) holds whenever

$$a\tan^2\alpha - 2b\tan\alpha + \Delta > 0, \quad \text{where} \tag{13}$$

$$a := \frac{\langle D''(\boldsymbol{r})\nabla D(\boldsymbol{r});\nabla D(\boldsymbol{r})\rangle}{\|\nabla D(\boldsymbol{r})\|^3} \quad \text{and} \tag{14}$$

$$b := \frac{|\langle D''(\boldsymbol{r})\Phi_{\frac{\pi}{2}}\nabla D(\boldsymbol{r});\nabla D(\boldsymbol{r})\rangle|}{\|\nabla D(\boldsymbol{r})\|^3}. \tag{15}$$

The solutions of (13) are given by

$$\tan\alpha < \chi(\boldsymbol{r}) := \begin{cases} a^{-1}[b - \sqrt{b^2 - a\Delta}] & \text{if } a\Delta \leq b^2 \\ +\infty & \text{otherwise.} \end{cases}$$

This is true, and so (10) does hold if $\chi(\boldsymbol{r}) = \infty\ \forall \boldsymbol{r}\in\widehat{W}$. Otherwise, invoking (11) shapes (13) into

$$0 < v_* < v \min_{\boldsymbol{r}\in\widehat{W}:\chi(\boldsymbol{r})<\infty} \frac{\chi(\boldsymbol{r})\|\nabla D(\boldsymbol{r})\|}{\sqrt{\chi(\boldsymbol{r})^2+1}}. \tag{16}$$

Modulo computation of the minima concerned, this and (9) explicitly describe the design parameters v_* for which the control objective is inevitably achieved. (If $\chi(\boldsymbol{r}) < \infty\ \forall \boldsymbol{r}\in\widehat{W}$, (9) and (16) are equivalent to (16).)

(iv) If the discontinuous control law (3) exhibits a sliding motion, the equivalent dynamics (Filippov, 1988) are addressed.

(v) Typically, the domain W expands towards $\boldsymbol{r}^0$ as $R_\star \downarrow$ due to (7) and (8). Since $\nabla D(\boldsymbol{r}^0) = 0$, this carries a potential of decreasing the upper bound of v_* recommended by (9) and (16). So, larger desired field growth rates v_* in (3) are compatible with worse steady error guarantees.

5. The isotropic distribution

Now we illustrate Theorem 4.1 in the simple yet instructive case of an isotropic distribution:

$$\begin{aligned} &D(\boldsymbol{r}) = \varphi(\|\boldsymbol{r}-\boldsymbol{r}^0\|), \quad \text{where } \varphi(p)\to 0 \text{ as } p\to\infty, \\ &\varphi(p)\geq 0, \qquad \varphi'(p) < 0 \quad \forall p > 0, \qquad \varphi'(0) = 0, \end{aligned} \tag{17}$$

and $\varphi(\cdot)$ is twice continuously differentiable. In particular, we show that the minima from (9) and (16) are reduced to those over one-dimensional intervals, which greatly simplifies their computation. Let an estimate of the distance from the vehicle initial location $\boldsymbol{r}_{\text{in}}$ to the unknown center $\boldsymbol{r}^0$ be available:

$$\|\boldsymbol{r}_{\text{in}} - \boldsymbol{r}^0\| \leq R_{\text{est}}. \tag{18}$$

To simplify matters, we assume that $R_{\text{est}} > R_\star + 4R$.

Assumption 3.1 is clearly fulfilled. The isolines are circles centered at $\boldsymbol{r}^0$. So the growth controllable points are those outside the disk of radius R centered at $\boldsymbol{r}^0$. Hence $\gamma_\star = \varphi(R_\star)$, $R_{\star\star} = R_\star$, and Assumption 3.2 reduces to $R_\star > 3R$.

Corollary 1. *Suppose that (17) and (18) hold, and that the required distance to the maximum point $R_\star > 3R$. Then the robot driven by the controller (3) reaches the desired vicinity (2) of the maximizer for a finite time and remains there afterwards provided that the controller parameter v_* is chosen from the intersection of the following two intervals:*

$$0 < v_* < v \min_{p\in[R_-,R_+]} |\varphi'(p)|, \qquad \begin{matrix} R_- := R_\star - 2R \\ R_+ := R_{\rm est} + 2R \end{matrix};$$

$$0 < v_* < v \min_{p\in[R_-,R_+]:\varphi''(p)\le 0} A(p), \quad \textit{where}$$

$$A(p) := \frac{|\varphi'(p)|}{\sqrt{1+\frac{R(R_\star-2R)|\varphi''(p)|}{(R_\star-3R)|\varphi'(p)|}}}, \tag{19}$$

and the minimum over the empty set is assumed to be $+\infty$.

Proof. We proceed from (iii) of Remark 4.1. By (8),

$$W \subset \widehat{W} := \{\boldsymbol{r} : R_\star - 2R \le \|\boldsymbol{r}-\boldsymbol{r}^0\| \le R_{\rm est} + 2R\}. \tag{20}$$

The isoline containing $\boldsymbol{r}$ is the circle of the radius $\|\boldsymbol{r}-\boldsymbol{r}^0\|$. Its signed curvature $\varkappa(\boldsymbol{r}) = -\|\boldsymbol{r}-\boldsymbol{r}^0\|^{-1}$. So, in (12),

$$\Delta = \min_{\boldsymbol{r}\in\widehat{W}} \left[\frac{1}{R} - \frac{1}{\|\boldsymbol{r}-\boldsymbol{r}^0\|}\right] = \frac{R_\star - 3R}{R(R_\star-2R)}. \tag{21}$$

Elementary computation shows that now $\|\nabla D(r)\| = |\varphi'(\|\boldsymbol{r}-\boldsymbol{r}^0\|)|$ and in (14) and (15),

$$a = \frac{\varphi''(\|\boldsymbol{r}-\boldsymbol{r}^0\|)}{|\varphi'(\|\boldsymbol{r}-\boldsymbol{r}^0\|)|}, \qquad b = 0.$$

It follows that (16) takes the form

$$0 < v_* < v \min_{\boldsymbol{r}\in\widehat{W}:\varphi''(p)\le 0} \frac{|\varphi'(p)|}{\sqrt{1+\frac{|\varphi''(p)|}{\Delta|\varphi'(p)|}}},$$

where $p := \|\boldsymbol{r}-\boldsymbol{r}^0\|$. By invoking (20) and (21), we arrive at the conclusion of the corollary. □

If a substance undergoes diffusion from an instantaneous pointwise source in an isotropic unbounded environment, its distribution profile at a given time is often Gaussian:

$$\varphi(p) = q\mathrm{e}^{-\frac{p^2}{2\sigma^2}}, \quad q > 0,\ \sigma > 0.$$

Given an estimate $q \ge q_- > 0$, (19) is implied by

$$0 < v_* < \frac{vq_-}{\sigma^2} \min_{r=R_-,R_+} r\mathrm{e}^{-\frac{r^2}{2\sigma^2}},$$

$$0 < v_* < \frac{q_- v}{\sigma^2} \begin{cases} +\infty & \text{if } \sigma < R_-; \quad \text{otherwise} \\ \dfrac{R_-\mathrm{e}^{-\frac{-R_-^2}{2\sigma^2}}}{\sqrt{1+\frac{RR_-}{R_- - R}\left[\frac{1}{R_-} - \frac{R_-}{\sigma^2}\right]}}. \end{cases} \tag{22}$$

Minimization of the right-hand sides in both lines from (22) over an estimated range of the dispersion $\sigma \in [\sigma_-, \sigma_+]$ provides an explicit description of the set of v_*'s for which the control objective achievement is guaranteed.

6. Proof of Theorem 4.1

We examine a robot driven by the control law (3). Since all inequalities from Assumption 3.2, (9) and (10) are strict, they remain true with $R_\star - \varepsilon$ put in place of $R_\star$ for $\varepsilon > 0, \varepsilon \approx 0$. Let W_ε be given by (8) with this substitution. We also introduce the vector $e = \mathbf{col}\,[\cos\theta, \sin\theta]$, and put

$$\sigma := \begin{cases} 0 & \text{if } \nabla D(\boldsymbol{r}) \text{ and } e \text{ are linearly dependent} \\ 1 & \text{if the angle from } \nabla D(\boldsymbol{r}) \text{ to } e \text{ is positive} \\ -1 & \text{if the angle from } \nabla D(\boldsymbol{r}) \text{ to } e \text{ is negative.} \end{cases}$$

The first lemma displays the major feature of the control law (3) that ultimately ensures achievement of the objective.

Lemma 6.1. *Within the region $W_\varepsilon = \{(\boldsymbol{r},\theta)\}$, the surface $\dot d = v_*$ is a barrier to penetration into the domain $\dot d < v_*$ as $t \uparrow$ whenever $\sigma = 1$ and into the domain $\dot d > v_*$ as $t \downarrow$ whenever $\sigma = -1$. If $\sigma = -1$, sliding motion along the surface does not hold, and starting on the surface, the robot either immediately enters the domain $\dot d > v_*$ with $u \equiv \overline{u}$ or remains in the domain $\dot d \le v_*$ with $u \equiv -\overline{u}$.*

Proof. Whenever the robot is on the surface $\dot d = v\langle\nabla D; e\rangle = v_*$, simple trigonometry shows that

$$e = \|\nabla D(r)\|^{-1}\Phi_{\sigma(\frac{\pi}{2}-\alpha)}\nabla D(r),$$

where α is given by (11). Hence

$$\begin{aligned} \ddot d = {} & v\langle\nabla D(\boldsymbol{r}); \dot e\rangle + v\langle D''(\boldsymbol{r})\dot r; e\rangle \\ \overset{(1)}{=\!=} {} & vu\langle\nabla D(\boldsymbol{r}); \Phi_{\frac{\pi}{2}} e\rangle + v^2\langle D''(\boldsymbol{r})e; e\rangle \\ = {} & vu\frac{\langle\nabla D(\boldsymbol{r}); \Phi_{\frac{\pi}{2}+\sigma(\frac{\pi}{2}-\alpha)}\nabla D(\boldsymbol{r})\rangle}{\|\nabla D(\boldsymbol{r})\|} \\ & + v^2\frac{\langle D''(\boldsymbol{r})\Phi_{\sigma(\frac{\pi}{2}-\alpha)}\nabla D(\boldsymbol{r}); \Phi_{\sigma(\frac{\pi}{2}-\alpha)}\nabla D(\boldsymbol{r})\rangle}{\|\nabla D(\boldsymbol{r})\|^2} \\ = {} & v^2\frac{\langle\nabla D(\boldsymbol{r}); \Phi_{-\sigma\alpha}\nabla D(\boldsymbol{r})\rangle}{\|\nabla D(\boldsymbol{r})\|} \\ & \times\left\{-\sigma\frac{u}{v} + \frac{\langle D''(\boldsymbol{r})\Phi_{\frac{\pi}{2}-\sigma\alpha}\nabla D(\boldsymbol{r}); \Phi_{\frac{\pi}{2}-\sigma\alpha}\nabla D(\boldsymbol{r})\rangle}{\|\nabla D(\boldsymbol{r})\|\langle\nabla D(\boldsymbol{r}); \Phi_{-\sigma\alpha}\nabla D(\boldsymbol{r})\rangle}\right\} \\ = {} & v^2\cos\alpha\|\nabla D(\boldsymbol{r})\| \\ & \times\left\{-\sigma\frac{u}{v} + \frac{\langle D''(\boldsymbol{r})\Phi_{\frac{\pi}{2}-\sigma\alpha}\nabla D(\boldsymbol{r}); \Phi_{\frac{\pi}{2}-\sigma\alpha}\nabla D(\boldsymbol{r})\rangle}{\cos(\sigma\alpha)\|\nabla D(\boldsymbol{r})\|^3}\right\}. \end{aligned} \tag{23}$$

By (6), $\Phi_\beta = \cos\beta I + \sin\beta\Phi_{\pi/2}$. So $\Phi_{\frac{\pi}{2}-\sigma\alpha}\nabla D(\boldsymbol{r}) = \Phi_{\frac{\pi}{2}}[\cos(\sigma\alpha)\nabla D(\boldsymbol{r}) - \sin(\sigma\alpha)\Phi_{\frac{\pi}{2}}\nabla D(\boldsymbol{r})]$, and the last ratio in (23) equals the right-hand side of (10), where in the last addend, $|\cdot|$ is dropped and $-2\sin\alpha$ is replaced by $+2\sin(\sigma\alpha)$. Now we examine the cases $\sigma = \pm 1$ separately.

Let $\sigma = 1$. Since $\dot d < v_* \overset{(3)}{\Rightarrow} u = -\overline{u}$ and whenever $u = -\overline{u}$, (10) and (23) imply that $\ddot d > 0$ at both the surface point at hand and, by continuity, in some of its vicinity, a move from this point into the set $\dot d - v_* < 0$ is impossible as $t \uparrow$. Now let $\sigma = -1$. Then in a vicinity of the surface point at hand, $\dot d > v_* \overset{(3)}{\Rightarrow} u = \overline{u} \Rightarrow \ddot d > 0$ by the same argument. This makes a move from this point into the set $\dot d > v_*$ impossible as $t \downarrow$, and justifies the last claim of the lemma. □

The next lemma shows that the robot reaches not only the desired vicinity (2) of the maximizer but also the closer vicinity $\{\boldsymbol{r} : \|\boldsymbol{r}-\boldsymbol{r}^0\| \le R_{\star\star}\} \overset{(7)}{\subset} V_\star$ and its subset, which is of interest to show that the robot will not leave $V_\star$ afterwards.

Lemma 6.2. *Let the robot state $\boldsymbol{r}, \theta$ at time $t = t_*$ be such that the circular path C traced from this state under $u \equiv -\overline{u}$ lies in the domain $W_{\min} := \{\boldsymbol{r} : D(\boldsymbol{r}) \ge \min\{\gamma_{\rm in}, \gamma_\star\}\}$. Then there exists a time $t_0 \ge t_*$ such that*

$$\boldsymbol{r}(t_0) \in V_{\star\star} := \{\boldsymbol{r} : \|\boldsymbol{r}-\boldsymbol{r}^0\| \le R_{\star\star} - 2R - \varepsilon\}, \tag{24}$$

and $D[\boldsymbol{r}(t)] \ge \min_{\boldsymbol{r}\in C} D[\boldsymbol{r}]$ for $t \in [t_*, t_0]$.

Proof. Let $t_0 := \min\{t \geq t_* : \boldsymbol{r}(t) \in V_{\star\star}\}$ and $t_0 := \infty$ if there are no such points t. If $t_0 = t_*$, the lemma trivially is true. For $t_0 > t_*$, we consider two cases separately.

(a) Let $u(t+0) = -\overline{u}\ \forall t \in [t_*, t_0)$. Then the robot moves along C for $t \in [t_*, t_0)$, and the claim of the lemma trivially holds if $t_0 < \infty$. Suppose that $t_0 = \infty$. Then a complete run over C is carried out, and $\|\boldsymbol{r}(t) - \boldsymbol{r}^0\| > R_{\star\star} - 2R - \varepsilon$ as $t \geq t_*$. Since $R_{\star\star} - 2R - \varepsilon > R$, the point r^0 is outside the disk D encircled by C, and so $\nabla D(\boldsymbol{r}) \neq 0\ \forall \boldsymbol{r} \in D$ by Assumption 3.1. Hence the boundary C of D contains a point $\overline{\boldsymbol{r}}$ where the gradient field is tangential to C and directed clockwise. At time $\overline{t} \geq t_*$, when $\boldsymbol{r}(\overline{t}) = \overline{\boldsymbol{r}}$, (9) implies that $\dot{d} = v\|\nabla D(\overline{\boldsymbol{r}})\| > v_*$, and so $u(\overline{t}) = \overline{u}$ by (3), in violation of (a). The contradiction obtained shows that $t_0 < \infty$.

(b) There exists $t \in [t_*, t_0)$ such that $u(t+0) \neq -\overline{u}$. We denote $t_1 := \max\{\overline{t} \in [t_*, t_0] : u(t+0) = -\overline{u}\ \forall t \in [t_*, \overline{t})\}$. Then $t_1 < \infty$ by the foregoing, $\boldsymbol{r}(t) \in C$ for $t \in [t_*, t_1]$, and $\dot{d}(t_1) \geq v_*$ by (3). Since $d(t) = D[\boldsymbol{r}(t)]$ is upper bounded, the inequality $\dot{d} \geq v_*$ cannot be kept true for all $t \geq t_1$; let $T := [t_1, t_+]$ be the maximal subinterval of $[t_1, t_0]$, where $\dot{d} \geq v_*$. Then $t \in T \Rightarrow D[\boldsymbol{r}(t)] \geq D[\boldsymbol{r}(t_1)] \geq \min_{\boldsymbol{r}\in C} D[\boldsymbol{r}]$ & $\boldsymbol{r}(t) \in W_\varepsilon$. So, if $t_+ = t_0$, the proof is completed. Suppose that $t_+ < t_0$. Then $\dot{d}(t_+) = v_*$, and, by (9), the vectors $e(t_+)$ and $\nabla D[\boldsymbol{r}(t_+)]$ are linearly independent: $\sigma(t_+) = \pm 1$. Due to Lemma 6.1, $\sigma(t_+) = -1$, $u(t) = -\overline{u}$ for $t > t_+, t \approx t_+$, and $\dot{d}(t) = v_*$ for $t_1 \leq t < t_+, t \approx t_+$. Let $T_* := [t_2, t_+]$ be the maximal interval with $t_2 \geq t_1$ such that $\dot{d}(t) = v_*\ \forall t \in T_*$. Then $\sigma(t) = -1\ \forall t \in T_*$, and Lemma 6.1 yields that $t_2 = t_1$, and so $u(t) = -\overline{u}$ for $t > t_1, t \approx t_1$, in violation of the definition of t_1. This contradiction shows that $t_+ = t_0$, thus completing the proof. □

Proof of Theorem 4.1. By applying Lemma 6.2 to $t_* := 0$, we see that, at some time $t = t_0$, the robot reaches the domain (24), which is a subset of (2) due to (7). Suppose that the robot leaves $V_\star$ for $t \geq t_0$, and consider the maximal time t_1 such that $\boldsymbol{r}(t) \in V_\star$ for all $t \in T = [t_0, t_1]$, and put $t_2 := \max\{t \in T : \boldsymbol{r}(t) \in V_{\star\star}\}$. Then $t_2 < t_1$ and $\boldsymbol{r}(t_*) \notin V_{\star\star}$ for $t_* > t_2, t_* \approx t_2$. Any circle C of the radius R passing through $\boldsymbol{r}(t_*)$ lies in the disk $\{\boldsymbol{r} : \|\boldsymbol{r} - \boldsymbol{r}^0\| \leq R_{\star\star} - \varepsilon/2\}$, where $D(\boldsymbol{r}) > \gamma_\star$ by (7). This permits us to apply Lemma 6.2 once more, which yields that $r(t_3) \in V_{\star\star}$ and $D[\boldsymbol{r}(t)] \geq \min_{\boldsymbol{r}\in C} D[\boldsymbol{r}] > \gamma_\star\ \forall t \in [t_*, t_3]$ for some $t_3 \geq t_*$. Here, $t_3 > t_1$ by the definition of t_2. So, by letting $t_* \to t_2 + 0$, we see that $D[\boldsymbol{r}(t)] \geq \gamma_\star$, and so $\boldsymbol{r}(t) \in V_\star$ due to (7) for all $t \in [t_2, t_3]$, in violation of the definition of t_1. The contradiction obtained completes the proof. □

7. Simulation results

We simulated a mobile robot modeled as a unicycle (1) with constant speed $v = 0.5$ m/s, time-varying angular velocity limited by $\overline{u} = 1$ rad/s, and minimal turning radius $R = 0.5$ m. The objective is to drive the robot within $R_\star = 3$ m distance from the location at which the field distribution attains its maximum. We examined a field with Gaussian distribution $D(x, y) = 10e^{-[(x-8)^2+(y-5)^2]/(2\sigma^2)}$, $\sigma^2 = 300$. In (3), the value $v_* := 0.05$ was taken within the range $0 < v_* < 0.0662$ that results from minimization of the right-hand sides in (22) (with $q_- = 5$, $\sigma_-^2 = 100$, $\sigma_+^2 = 500$, $R_{est} = 9$ m), as is recommended at the end of Section 5. The robot approaches the required $R_\star$-neighborhood $V_\star$ of the maximizer along a spiral-like trajectory, as is shown in Figs. 1 and 2. (In Fig. 1, the concentric circles depict the field level sets; $V_\star$ is bounded by the smallest of them.) The distance from the robot to the maximizer first decays monotonically and then stays within the predefined margin. Within $V_\star$, the robot keeps moving along a circle with radius R by applying the maximal steering angle $u \equiv \overline{u}$. Other simulations showed that an increase of v_* within the range given by (22) causes a decrease of the average curvature of the robot path. Though our main theorem concerns steady distributions, the algorithm works well for moving sources. Fig. 3 concerns the case where the source (i.e., the center of the above Gaussian distribution) moves at the speed 0.05 m/s along the blue curve. The robot still approaches the source and then maintains the required accuracy, while circulating around the source.

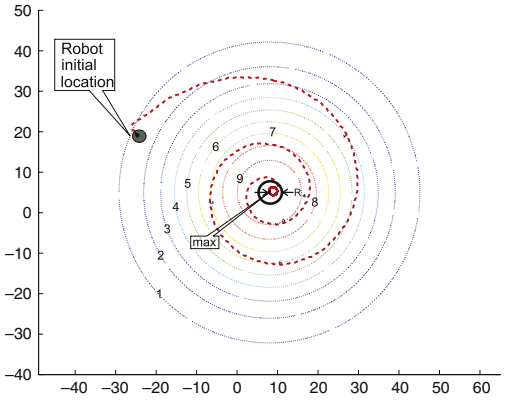

Fig. 1. The robot trajectory towards the maximizer.

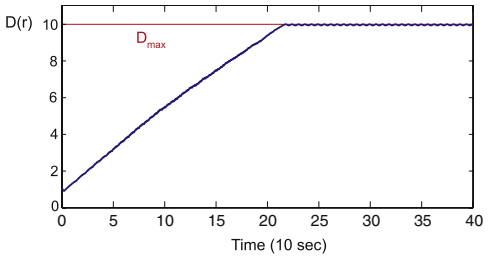

Fig. 2. Field distribution value at the robot position.

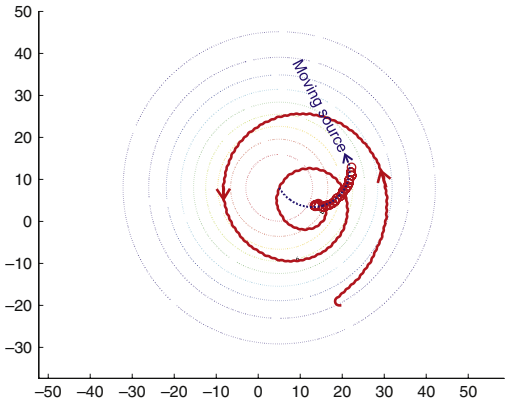

Fig. 3. The robot tracking a moving source.

Figs. 4 and 5 concern another case not covered by the main theorem: the case of the distribution $D(x, y) = 10e^{-\frac{(x-10)^2+(y-8)^2}{600}} + 18e^{-\frac{(x+20)^2+(y+12)^2}{200}}$ with two local maxima depicted by $*$ and $+$, where $*$ corresponds to the global maximum. The control law (3) exhibits behavior typical for numerical optimization methods driven by local information about the cost function (see, e.g., Nocedal and Wright (1999)). When started sufficiently close to a particular local maximizer, the robot converges to it. In general, the robot converges to the extremum whose domain of attraction it enters during the motion. Though analogy with numerical methods (Nocedal & Wright, 1999) underlies a possibility of more complicated behaviors, they were not encountered in our simulations.

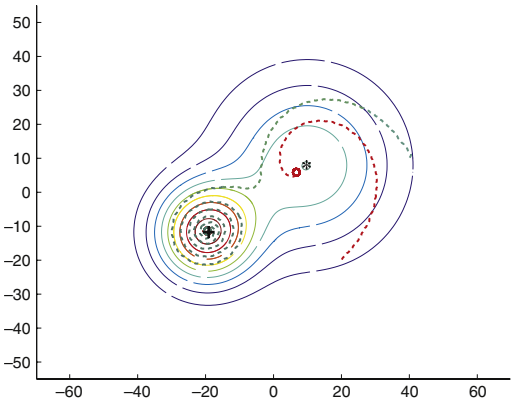

Fig. 4. Trajectories in the case of multiple maxima; $v_* = 0.1$.

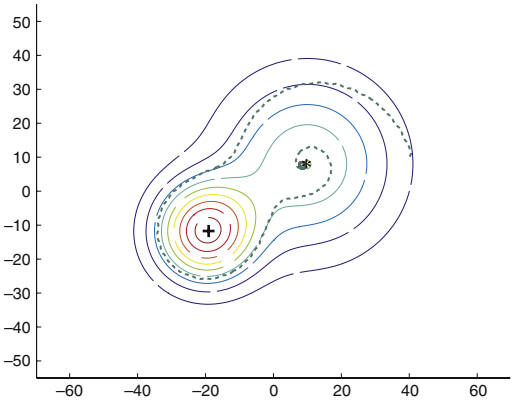

Fig. 5. Trajectory in the case of multiple maxima; $v_* = 0.05$.

We also examined the robustness of the proposed control law against numerical differentiation errors in conjunction with the measurement noise. The estimation of derivatives from noise-corrupted data is a well-established discipline, which offers a variety of approaches. They include approximation of the transfer function of the ideal differentiator, optimal differentiation based on stochastic models, observers with sliding modes and large gains, difference methods, and approximation and Tikhonov regularization (see, e.g., Ahnert and Abel (2007) and Vasiljevic and Khalil (2008) for recent surveys). To examine the worst-case scenario, the simplest two-point finite difference derivative estimate was used. Measurements were corrupted by a Gaussian white noise with zero mean and standard deviation $\sigma = 0.03$ (which was chosen with regard to the range of d concerned and typical accuracies of modern sensors for concentration, magnetism, temperature, etc.). As is shown in Fig. 6, the robot moves close to the 'noise-free' trajectory and ultimately maintains the required range accuracy. Fig. 7 illustrates the influence of the time constant τ used to estimate the derivative $\dot{d}(t) \approx \tau^{-1}[d(t) - d(t-\tau)]$. The implications of the related errors are almost invisible as τ ranges from 0.1 to 1.0 s. Slight chattering occurs for $\tau = 1.8$ s (with the space amplitude ≈0.4 m, i.e., ≈44% of the distance covered by the robot for τ seconds at the speed 0.5 m/s). This confirms the reputation of sliding-mode controllers as tolerable to noise and errors.

Fig. 8 illustrates the case where (3) is replaced by a similar linear controller with saturation $u(t) = \max\{-\bar{u}; \min\{\bar{u}; \tan(\alpha) \cdot [\dot{d} - v_*]\}\}$, where $\tan(\alpha)$ is the gain coefficient and saturation is due to the constraint $|u| \le \bar{u}$ from (1). (This control law converts into (3) as $\alpha \to \infty$.) As is illustrated by Fig. 8, the performance is monotonically improved as the gain coefficient increases. The

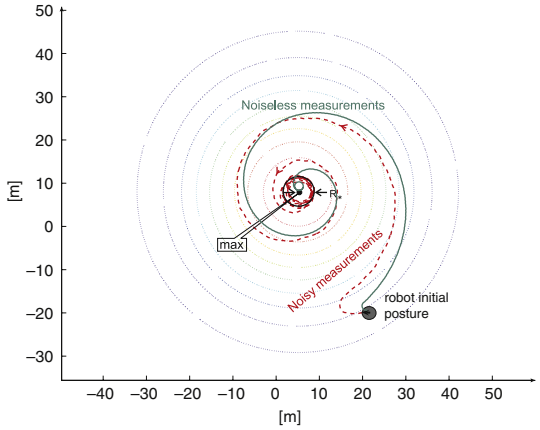

Fig. 6. Trajectories for noiseless and noisy measurements.

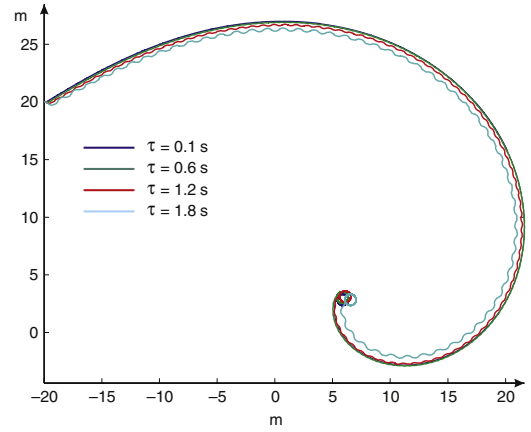

Fig. 7. Influence of differentiation constant.

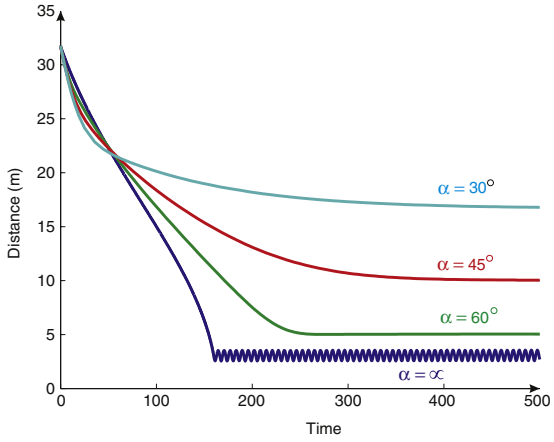

Fig. 8. Control by linear controllers with saturation.

required ultimate distance 3 m to the maximizer is achieved for slopes $\alpha \gtrapprox 75°$ for which the law at hand can be viewed as a fairly close approximation of the discontinuous rule (3). This does not come as a surprise, since non-holonomic robots like (1) are typically not controllable by linear controllers (Brockett, 1983) due to deficiency of controllability of their linear models. The above facts partly explain our initial interest in the discontinuous controller (3). Detailed study of the capabilities of linear controllers is also of interest, and we consider this as a topic of future work.

Appendix. Proof of Proposition 3.1

If $\dot d \overset{(1)}{=\!=} v\langle \nabla D[\boldsymbol{r}]; e\rangle = 0$, then $e = \frac{\Phi_{\sigma\frac{\pi}{2}}\nabla D(\boldsymbol{r})}{\|\nabla D(\boldsymbol{r})\|}$, $\sigma = \pm 1$, and

$$\begin{aligned}
\ddot d &= v\langle \nabla D(\boldsymbol{r}); \dot e\rangle + v\langle D''(\boldsymbol{r})\dot r; e\rangle \\
&\overset{(1)}{=\!=} vu\langle \nabla D(r); \Phi_{\frac{\pi}{2}} e\rangle + v^2\langle D''(\boldsymbol{r})e; e\rangle \\
&= vu\frac{\langle \nabla D(\boldsymbol{r}); \Phi_{(\sigma+1)\frac{\pi}{2}}\nabla D(\boldsymbol{r})\rangle}{\|\nabla D(\boldsymbol{r})\|} \\
&\quad + v^2\frac{\langle D''(r)\Phi_{\sigma\frac{\pi}{2}}\nabla D(\boldsymbol{r}); \Phi_{\sigma\frac{\pi}{2}}\nabla D(\boldsymbol{r})\rangle}{\|\nabla D(\boldsymbol{r})\|^2} \\
&= \|\nabla D(\boldsymbol{r})\|v^2\left\{-\frac{u}{v}\sigma + \frac{\langle D''(r)\Phi_{\frac{\pi}{2}}\nabla D(\boldsymbol{r}); \Phi_{\frac{\pi}{2}}\nabla D(\boldsymbol{r})\rangle}{\|\nabla D(\boldsymbol{r})\|^3}\right\};
\end{aligned}$$

$$\max_{u:|u|\le\bar u} \ddot d = \|\nabla D(\boldsymbol{r})\|v^2\{\varkappa_{\text{veh}} + \varkappa(\boldsymbol{r})\},$$

which completes the proof. □

References

Ahnert, K., & Abel, M. (2007). Numerical differentiation of experimental data: local versus global methods. *Computer Physics Communications*, *177*, 764–774.

Ariyur, K. B., & Krstic, M. (2003). *Real-time optimization by extremum-seeking feedback*. Hoboken, NJ: Wiley-Interscience.

Bachmayer, R., & Leonard, N. E. (December 2002). Vehicle networks for gradient descent in a sampled environment. In *Proc. of the 41st IEEE CDC* (pp. 113–117).

Biyik, E., & Arcak, M. (December 2007). Gradient climbing in formation via extremum seeking and passivity-based coordination rules. In *Proc. of the 46th IEEE CDC* (pp. 3133–3138).

Brockett, R. W. (1983). Asymptotic stability and feedback stabilization. In R. W. Brockett, R. S. Millman, & H. J. Sussmann (Eds.), *Differential geometric control theory* (pp. 181–191).

Burian, E., Yoeger, D., Bradley, A., & Singh, H. (June 1996). Gradient search with autonomous underwater vehicle using scalar measurements. In *Proc. of the IEEE symposium on underwater vehicle technology* (pp. 86–98).

Cochran, J., & Krstic, M. (2009). Nonholonomic source seeking with tuning of angular velocity. *IEEE Transactions on Automatic Control*, *54*, 717–731.

Edwards, C., Fossas, C. E., & Fridman, L. (Eds.). (2006). *Advances in variable structure and sliding mode control*. Berlin: Springer.

Filippov, A. F. (1988). *Differential equations with discontinuous righthand sides*. Kluwer Academic Publishers.

Gazi, V., & Passino, K. M. (2004). Stability analysis of social foraging swarms. *IEEE Transactions on Systems, Man and Cybernetics*, *54*, 539–557.

Horst, R., & Pardalos, P. M. (Eds.). (1995). *Handbook of global optimization*. Dordrecht: Kluwer Academic Publishers.

Lee, H., Utkin, V. I., & Malinin, A. (2009). Chattering reduction using multiphase sliding mode control. *International Journal of Control*, *82*, 1720–1737.

Manchester, I. R., & Savkin, A. V. (2004). Circular navigation guidance law with incomplete information and uncertain autopilot model. *Journal of Guidance, Control and Dynamics*, *27*(6), 1076–1083.

Manchester, I. R., & Savkin, A. V. (2006). Circular navigation guidance law for precision missile target engagement. *Journal of Guidance, Control and Dynamics*, *29*(2), 314–320.

Nocedal, J., & Wright, S. (1999). Numerical optimization. In *Springer series in operations research and financial engineering*. New York: Springer-Verlag.

Ögren, P., Fiorelli, E., & Leonard, N. E. (2004). Cooperative control of mobile sensor networks: adaptive gradient climbing in a distributed environment. *IEEE Transactions on Automatic Control*, *49*, 1292–1301.

Porat, B., & Neohorai, A. (1996). Localizing vapor-emitting sources by moving sensors. *IEEE Trans. Signal Processing*, *44*, 1018–1021.

Teimoori, H., & Savkin, A. V. (2010). Equiangular navigation and guidance of a wheeled mobile robot based on range-only measurements. *Robotics and Autonomous Systems*, *58*, 203–215.

Utkin, V. I. (1992). *Sliding modes in control optimization*. Berlin: Springer-Verlag.

Vasiljevic, L. K., & Khalil, H. K. (2008). Error bounds in differentiation of noisy signals by high-gain observers. *Systems & Control Letters*, *57*, 856–862.

Zhang, Ch., Arnold, D., Ghods, N., Siranosian, A., & Krstic, M. (2007). Source seeking with non-holonomic unicycle without position measurement and with tuning of forward velocity. *Systems & Control Letters*, *56*, 245–252.

Alexey S. Matveev was born in Leningrad, USSR, in 1954. He received his M.S. and Ph.D. degrees in 1976 and 1980, respectively, both from Leningrad University. Currently, he is a Professor in the Department of Mathematics and Mechanics, Saint Petersburg University. His research interests include estimation and control over communication networks, hybrid dynamical systems, and navigation and control of mobile robots.

Hamid Teimoori was born in 1978 in Iran. He received his B.Sc. degree (Hons 1) in 2000 from Ferdowsi University, M.Sc. degree (2002) from Iran University of Science and Technology, Tehran, Iran and Ph.D. degree (2009) in Electrical Engineering from the University of New South Wales (UNSW), Sydney, Australia. From 2002 to 2005, he worked as an Associate Lecturer in Imam-Reza University, Iran. He is currently a Research Associate at the University of New South Wales. His research interests currently center on non-holonomic systems and navigation and guidance of wheeled robots and unmanned aerial vehicles.

Andrey V. Savkin was born in 1965 in Norilsk, USSR. He received his M.S. and Ph.D. degrees from Leningrad State University, USSR, in 1987 and 1991, respectively. From 1987 to 1992, he was with the Television Research Institute, Leningrad, USSR. From 1992 to 1994, he held a postdoctoral position in the Department of Electrical Engineering, Australian Defence Force Academy, Canberra. From 1994 to 1996, he was a Research Fellow with the Department of Electrical and Electronic Engineering and the Cooperative Research Center for Sensor Signal and Information Processing at the University of Melbourne, Australia. From 1996 to 2000, he was a Senior Lecturer, and then an Associate Professor, in the Department of Electrical and Electronic Engineering at the University of Western Australia, Perth. Since 2000, he has been a Professor at the School of Electrical Engineering and Telecommunications at the University of New South Wales, Sydney, Australia.

His current research interests include robust control and state estimation, hybrid dynamical systems, guidance, navigation and control of mobile robots, applications of control, and signal processing in biomedical engineering and medicine.

He has authored/co-authored five research monographs and numerous journal and conference papers on these topics. He has served as an associate editor for several international journals.